

Nonlinear dynamics of system oscillations modeled by a forced Van der Pol generalized oscillator

L. A. Hinv^{*}, C. H. Miwadinou[†], A. V. Monwanou[‡] and
J. B. Chabi Orou[§]

Abstract

This paper considers the oscillations modeled by a forced Van der Pol generalized oscillator. These oscillations are described by a nonlinear differential equation of the form $\ddot{x} + x - \varepsilon(1 - ax^2 - bx^2)\dot{x} = E \sin \Omega t$. The amplitudes of the forced harmonic, primary resonance superharmonic and subharmonic oscillatory states are obtained using the harmonic balance technique and the multiple time scales methods. We obtain also the hysteresis and jump phenomena in the system oscillations. Bifurcation sequences displayed by the model for each type of oscillatory states are performed numerically through the fourth-order Runge-Kutta scheme.

Keywords : Van der Pol generalized oscillator, forced harmonic, resonance states, bifurcation, Lyapunov exponent and chaoticity basin.

1 Introduction

Many problems in physics, chemistry, biology, etc., are related to nonlinear self-excited oscillators ([1] - [2]). Thus, Balthazar Van der Pol (1889 – 1959) was a Dutch electrical engineer who initiated modern experimental dynamics in the laboratory during the 1920's and 1930's. He, first, introduced his (now famous) equation in order to describe triode oscillations in electrical circuits, in 1927 ([3]- [14]). The mathematical model for the system is a well known second order ordinary differential equation with cubic nonlinearity Van der Pol equation. Since then thousands of papers have been published achieving better approximations to the solutions occurring in such non linear systems. The Van der Pol oscillator is a classical example of self-oscillatory system and is now considered as very useful mathematical model that can be used in much more complicated and modified systems. But, why this equation is so important to mathematicians, physicists and engineers and is still being extensively studied?

During the first half of the twentieth century, Balthazar Van der Pol pioneered the fields of radio and telecommunications [3]. In an era when these areas were much less advanced than they are today, vacuum tubes were used to control the flow of electricity

^{*}laurent.hinvi@imsp-uac.org

[†]clement.miwadinou@imsp-uac.org, hodevewan@yahoo.fr

[‡]movins2008@yahoo.fr

[§]Author to whom correspondence should be addressed: jchabi@yahoo.fr

in the circuitry of transmitters and receivers. Contemporary with Lorenz, Thompson, and Appleton, Van der Pol, in 1927, experimented with oscillations in a vacuum tube triode circuit and concluded that all initial conditions converged to the same periodic orbit of finite amplitude. Since this behavior is different from the behavior of solutions of linear equations, Van der Pol proposed a nonlinear differential equation

$$\ddot{x} + x - \varepsilon(1 - x^2)\dot{x} = 0, \quad (1)$$

commonly referred to as the (unforced) Van der Pol equation [4], as a model for the behavior observed in the experiment. In studying the case $\varepsilon \gg 1$, Van der Pol discovered the importance of what has become known as relaxation oscillations ([5], [11]). Van der Pol went on to propose a version of (1) that includes a periodic forcing term [9]:

$$\ddot{x} + x - \varepsilon(1 - x^2)\dot{x} = E \sin \Omega t. \quad (2)$$

Many systems have characteristics of two types of oscillators and whose equation presents a combination of terms of these oscillators. Thus, we have the systems characterized by Van der Pol and Rayleigh oscillators namely the Van der Pol generalized oscillator [13] or hybrid Van der pol-Rayleigh oscillator modeled by

$$\ddot{x} + x - \varepsilon(1 - ax^2 - bx^2)\dot{x} = 0. \quad (3)$$

The Van der Pol generalized oscillator as all oscillator, models many physical systems. Thus, we have [14] who models a bipedal robot locomotion with this oscillator "known as Hybrid Van der Pol-Rayleigh oscillators".

In the present paper, We considered the forced Van der Pol generalized oscillator equation [13]

$$\ddot{x} + x - \varepsilon(1 - ax^2 - bx^2)\dot{x} = E \sin \Omega t, \quad (4)$$

where a, b are positifs cubic nonlinearities, $\varepsilon \ll 1$ is damping parameters while E and Ω stand for the amplitude and the pulsation of the external excitation.

We concentrate our studies on the equation of motion (4), the resonant states, the chaotic behavior. Through these studies, we found the effects of differents parameters in general.

The paper is structured as follows: Section 2 gives an analytical treatment of equation (4). Amplitude of the forced harmonic oscillatory states is obtained with harmonic-balance method [15]. Section 3 investigate using multiple time-scales method [16] the resonant cases and the stability conditions are found by the perturbation method [15]. The section 4 evaluates bifurcation and chaotic behavior by numerically simulations of equation (4). Section 5 deals with conclusions.

2 Amplitude of the forced harmonic oscillatory states

Assuming that the fundamental component of the solution and the external excitation have the same period, the amplitude of harmonic oscillations can be tackled using the harmonic balance method ([15]). For this purpose, we express its solutions as

$$x = A \sin \Omega t + \xi \quad (5)$$

where A represents the amplitude of the oscillations and $\xi \ll 1$ a constant. Inserting this solution (5) in (4) we obtain

$$(1 - \Omega^2)A \sin \Omega t + \xi + \varepsilon \left[(1 - a\xi^2)A\Omega - \frac{aA^3\Omega}{4} - \frac{3bA^3\Omega^3}{4} \right] \cos \Omega t + \varepsilon \frac{(aA^3\Omega - bA^3\Omega^3)}{4} \cos 3\Omega t - \varepsilon \xi a A^2 \sin 2\Omega t = E \sin \Omega t. \quad (6)$$

By equating the constants and the coefficients of $\sin \omega$ and $\cos \omega$, we have

$$(1 - \Omega^2)A = E, \quad (7)$$

$$\xi = 0, \quad (8)$$

$$\varepsilon \left[(1 - a\xi^2)A\Omega - \frac{aA^3\Omega}{4} - \frac{3bA^3\Omega^3}{4} \right] = 0 \quad (9)$$

\Leftrightarrow

$$(1 - \Omega^2)^2 A^2 = E^2, \quad (10)$$

$$\varepsilon^2 \left[(1 - a\xi^2)A\Omega - \frac{aA^3\Omega}{4} - \frac{3bA^3\Omega^3}{4} \right]^2 = 0. \quad (11)$$

We combined the Equations (10 -11) and we obtain

$$[(1 - \Omega^2)^2 - \varepsilon^2 \Omega^2] A^2 + \frac{\varepsilon^2 \Omega^2}{2} (a + 3b\Omega^2) A^4 - \frac{\varepsilon^2 \Omega^2}{16} (a + 3b\Omega^2)^2 A^6 = E^2. \quad (12)$$

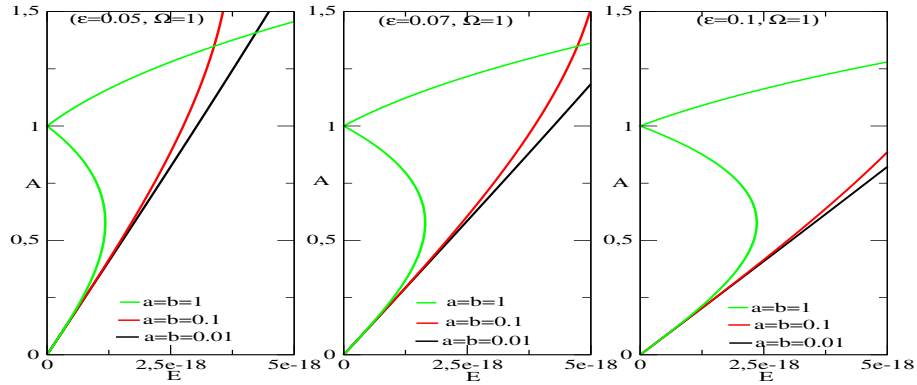


Figure 1: Effects of the parameters a, b, ε on the amplitude-response curves with $\Omega = 1$.

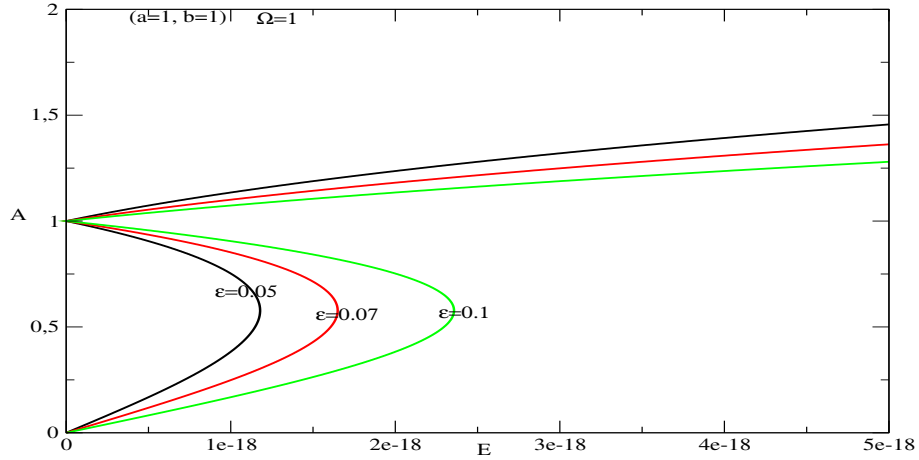


Figure 2: Effects of the parameter ε on the amplitude-response curves with $a = b = 1, \Omega = 1$.

The figures 1 and 2 show the effects of the parameters a, b, ε on the amplitude-response curves $A(E)$. Through these figures, we note that for small value of Rayleigh coefficient a and Van der Pol coefficient b the amplitude-response is linear and when its increase, the hysteresis and jump phenomena appear. The gap of jump phenomenon decreases when the damping parameter ε increases but hysteresis and jump phenomena persist.

3 Resonant states

We investigate the different resonances with the Multiple time scales Method *MSM*. In such a situation, an approximate solution is generally sought as follows:

$$x(\varepsilon, t) = x_0(T_0, T_1) + \varepsilon x_1(T_0, T_1) + \dots \quad (13)$$

With $T_n = \varepsilon^n t$.

The derivatives operators can now be rewritten as follows:

$$\begin{cases} \frac{d}{dt} = D_0 + \varepsilon D_1 + \dots \\ \frac{d^2}{dt^2} = D_0^2 + 2\varepsilon D_0 D_1 + \dots \end{cases} \quad (14)$$

where $D_n^m = \frac{\partial^m}{\partial T_n^m}$.

3.1 Primary resonant state

In this state, we put that $E \propto \varepsilon \tilde{E}$. The closeness between both internal and external frequencies is given by $\Omega = 1 + \varepsilon \sigma$. Where $\sigma = o(1)$ is the detuning parameter, the internal frequency is 1. Inserting (13) and (14) into (4) we obtain:

$$\begin{aligned} & (D_0^2 + 2\varepsilon D_0 D_1) (x_0 + \varepsilon x_1) + x_0 + \varepsilon x_1 - \varepsilon E \sin \Omega t = \\ & \varepsilon \left[1 - a(x_0 + \varepsilon x_1)^2 - b[(D_0 + \varepsilon D_1)(x_0 + \varepsilon x_1)]^2 \right] (D_0 + \varepsilon D_1)(x_0 + \varepsilon x_1). \end{aligned} \quad (15)$$

Equating the coefficients of like powers of ϵ after some algebraic manipulations, we obtain:

$$\begin{cases} D_0^2 x_0 + x_0 = 0, \\ D_0^2 x_1 + x_1 = E \sin \Omega t - 2D_1 D_0 x_0 + (1 - ax_0^2 - b(D_0 x_0)^2) D_0 x_0. \end{cases} \quad (16)$$

The general solution of the first equation of system (16) is

$$x_0 = A(T_1) \exp(jT_0) + CC, \quad (17)$$

where CC represents the complex conjugate of the previous terms. $A(T_1)$ is a complex function to be determined from solvability or secular conditions of the second equation of system (16). Thus, substituting the solution x_0 in (16) leads us to the following secular criterion

$$\begin{aligned} D_0^2 x_1 + x_1 &= j \left[-2A' + (1 - a|A|^2 - 3b|A|^2) A \right] e^{jT_0} + j(b-a) A^3 e^{3jT_0} + \\ &\quad - \frac{jE}{2} e^{j(1+\epsilon\sigma)t} + CC \\ &= j \left[-2A' + (1 - (a+3b)|A|^2) A - \frac{E}{2} e^{j\sigma\epsilon t} \right] e^{jT_0} + \\ &\quad + j(b-a) A^3 e^{3jT_0} + CC. \end{aligned} \quad (18)$$

The secular criterion follows

$$\left[-2A' + A - (a+3b)|A|^2 A - \frac{E}{2} e^{j\sigma T_1} \right] = 0. \quad (19)$$

In polar coordinates, the solution of (19) is

$$A = \frac{1}{2} p(T_1) \exp[j\theta(T_1)], \quad (20)$$

where p and θ are real quantities and stand respectively for the amplitude and phase of oscillations. After injecting (20) into (19), we obtain

$$-p' - j\theta'p + \frac{1}{2}p - \frac{(a+3b)p^3}{8} - \frac{E}{2} e^{j(\sigma T_1 - \theta(T_1))} = 0. \quad (21)$$

We separate real and imaginary terms and obtain the following coupled flow for the amplitude and phase:

$$\begin{cases} -p' + \frac{1}{2}p - \frac{(a+3b)p^3}{8} = \frac{E}{2} \cos \Phi \\ -\Phi'p + p\sigma = \frac{E}{2} \sin \Phi, \end{cases} \quad (22)$$

where the prime denotes the derivative with respect to T_1 and $\Phi = \sigma T_1 - \theta(T_1)$. For the steady-state conditions ($p' = \Phi' = 0 \Leftrightarrow p = p_0, \Phi = \Phi_0$), the following nonlinear algebraic equation is obtained:

$$\left(\frac{1+4\sigma^2}{4} \right) p_0^2 - \frac{a+3b}{8} p_0^4 + \frac{(a+3b)^2}{64} p_0^6 = \frac{E^2}{4}, \quad (23)$$

where p_0 and Φ_0 are respectively the values of p and Φ in the steady-state. Eq.(23) is the equation of primary resonance flow. Now, we study the stability of the process, we assume that each equilibrium state is submitted to a small perturbation as follows

$$\begin{cases} p = p_0 + p_1 \\ \Phi = \Phi_0 + \Phi_1 \end{cases} \quad (24)$$

where p_1 and Φ_1 are slight variations. Inserting the equations (24) into (22) after some algebraic and canceling nonlinear terms enable us to obtain

$$p'_1 = -\frac{1}{2} \left[1 + 3 \frac{(a+3b)p_0^2}{4} \right] p_1 - p_0 \sigma \Phi_1, \quad (25)$$

$$\Phi'_1 = \frac{\sigma}{p_0} p_1 - \frac{1}{2} \left[1 - \frac{(a+3b)p_0^2}{4} \right] \Phi_1 \quad (26)$$

The stability process depends on the sign of eigenvalues Γ of the equations (25) and (26) which are given through the following characteristic equation

$$\Gamma^2 + 2Q\Gamma + R = 0, \quad (27)$$

where

$$\begin{cases} Q = \frac{1}{2} \left(1 + \frac{(a+3b)p_0^2}{4} \right) \\ R = \frac{1}{4} \left(1 + 3 \frac{(a+3b)p_0^2}{4} \right) \left(1 - \frac{(a+3b)p_0^2}{4} \right) - \sigma^2. \end{cases}$$

Since $Q > 0$, the steady-state solutions are stable if $R > 0$ and unstable otherwise.

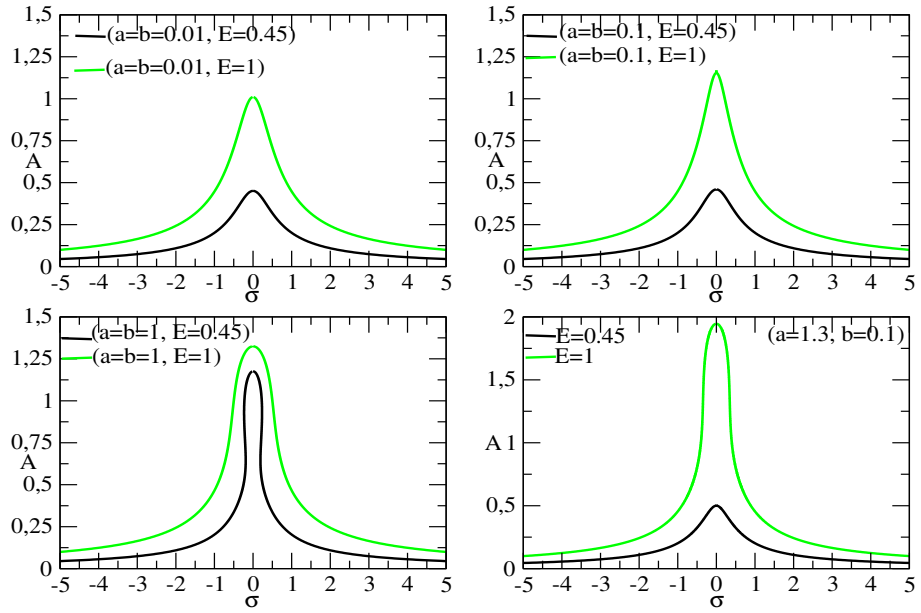


Figure 3: Effects of the parameters a, b, E on primary resonance curves

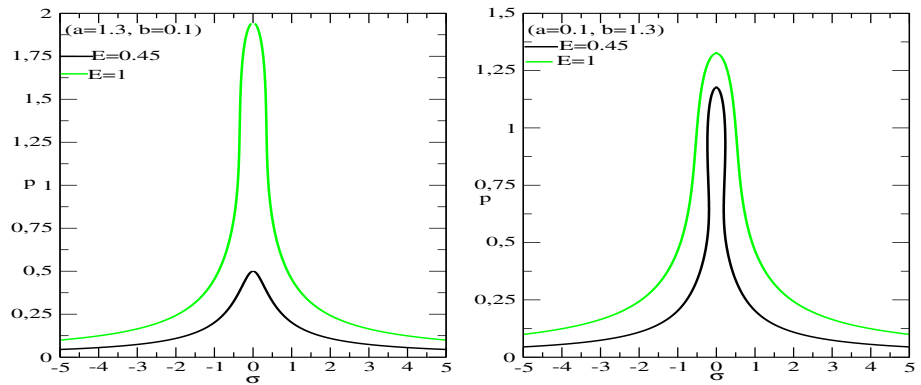


Figure 4: Effects of the parameters a, b, E on the primary resonance curves

The figures 3 and 4 display the primary resonance curves obtained from (23) for different values of the parameters a, b, E . We obtained the linear resonances curves and we found that resonance amplitude increase when the external forced amplitude increase. Through these figures we found also the peak value of resonance amplitude is higher when $a + 3b > 1$ than $a + 3b < 1$.

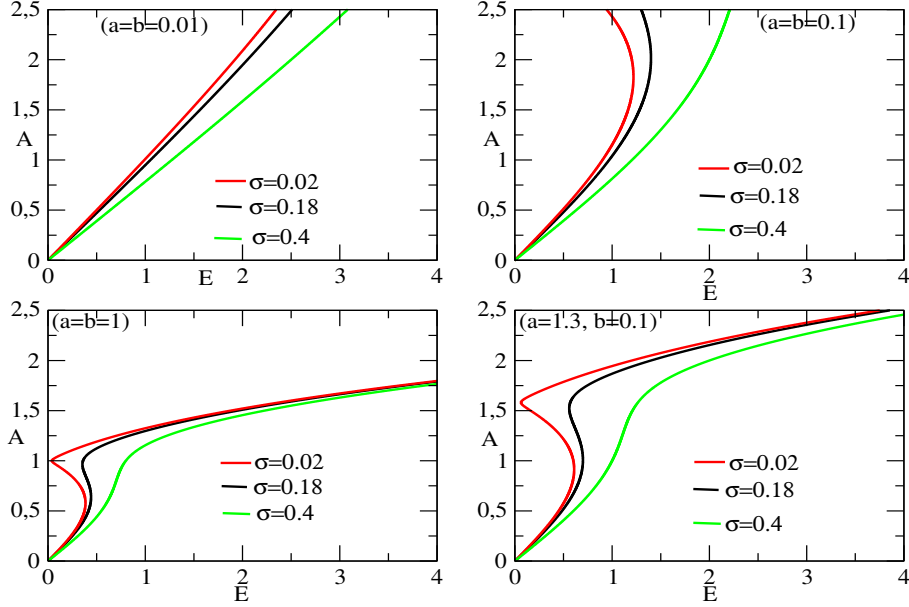


Figure 5: Effects of the parameters a, b, σ on the amplitude-response curves

The figure 5 displays the amplitudes response curves obtained from (23) for different values of the parameters a, b, σ . We obtained for $a+3b \ll 1$ the amplitude-response that is linear function of E and the slope decreases as the σ increases. The hysteresis's phenomena appears when $a + 3b$ is important for small value of σ and disappears when σ increases.

3.2 Superharmonic and subharmonic oscillations

When the amplitude of the sinusoidal external force is large, other type of oscillations can be displayed by the model, namely the superharmonic and the subharmonic oscillatory states. It is now assumed that $E \propto \varepsilon^0 \bar{E}$ and therefore, one obtains the following equations at different order of ε . In order ε^0 ,

$$D_0^2 x_0 + x_0 = E \sin(\Omega T_0). \quad (28)$$

In order ε^1 ,

$$D_0^2 x_1 + x_1 = -2D_1 D_0 x_0 + (1 - ax_0^2 - b(D_0 x_0)^2) D_0 x_0. \quad (29)$$

The general solution of Eq.(29) is

$$\begin{cases} x_0 = A(T_1)e^{jT_0} + \Lambda e^{j\Omega T_0}, \\ \text{with } \Lambda = \frac{E}{2(1-\Omega^2)}. \end{cases} \quad (30)$$

Substituting the general solution x_0 into Eq. (29), after some algebraic manipulations, we obtain

$$\begin{aligned}
D_0^2 x_1 + x_1 = & j [-2A' + A (1 - (a + 3b) |A|^2) - 2A\Lambda^2 (a + 3b\Omega^2)] e^{jT_0} + \\
& + j [\Lambda\Omega - 2(a + 3b) |A|^2 \Lambda\Omega - \Lambda^3 \Omega (a + 3b\Omega^2)] e^{j\Omega T_0} + \\
& + j(b - a) A^3 e^{3jT_0} + j\Lambda^3 \Omega (b\Omega^2 - a) e^{3j\Omega T_0} + \\
& + j [-a(1 + 2\Omega) + 3b\Omega^2] A\Lambda^2 e^{j(1+2\Omega)T_0} + \\
& + j [-a(2 + \Omega) + 3b\Omega] A^2 \Lambda e^{j(2+\Omega)T_0} + \\
& + j [a(2 - \Omega) + 3b\Omega] A^2 \Lambda e^{j(\Omega-2)T_0} \\
& + j [a(2\Omega - 1) + 3b\Omega] A\Lambda^2 e^{j(1-2\Omega)T_0} + CC, \tag{31}
\end{aligned}$$

where CC represents the complex conjugate of the previous terms.

From Eq.(31), it comes that superharmonic and subharmonic states can be found from the quadratic and cubic nonlinearities. The cases of superharmonic oscillation we consider is $3\Omega = 1 + \epsilon\sigma$, while the subharmonic oscillation to be treated is $\Omega = 3 + \epsilon\sigma$.

3.2.1 Superharmonic states

For the first superharmonic states $3\Omega = 1 + \epsilon\sigma$, equating resonant terms at 0 from Eq.(31), we obtain:

$$-2A' + A [1 - (a + 3b)|A|^2 - 2\Lambda^2(a + 3b\Omega^2)] + \Lambda^3 \Omega (\Omega^2 b - a) e^{j\epsilon\sigma T_0} = 0. \tag{32}$$

Using (20) and after some algebraic manipulations, we rewrite (32) as follows

$$\begin{cases} p' = \frac{p}{2} \left[1 - \frac{p^2}{4}(a + 3b) - 2\Lambda^2(a + 3b\Omega^2) \right] + \Lambda^3 \Omega (b\Omega^2 - a) \cos \Phi, \\ p\Phi' = p\sigma - \Lambda^3 \Omega (b\Omega^2 - a) \sin \Phi, \text{ with } \Phi = \sigma T_1 - \theta. \end{cases} \tag{33}$$

The amplitude of oscillations of this superharmonic states ($p' = \Phi' = 0 \Leftrightarrow p = p_0, \Phi = \Phi_0$) is governed by the following nonlinear algebraic equation

$$\begin{cases} \frac{(a+3b)^2}{64} p_0^6 - \mu \frac{a+3b}{4} p_0^4 + (\mu^2 + \sigma^2) p_0^2 - \Lambda^6 \Omega^2 (a - b\Omega^2)^2 = 0, \\ \text{with } \mu = \frac{1}{2} - \Lambda^2 (a + 3\Omega^2 b). \end{cases} \tag{34}$$

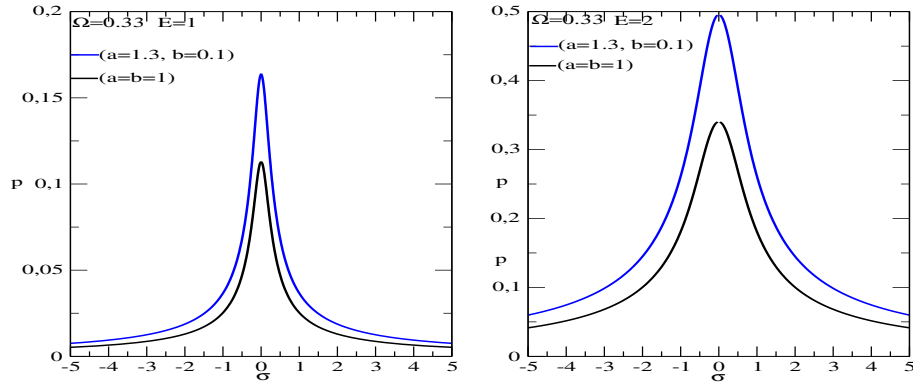


Figure 6: Effects of the parameters a, b, E on the superharmonic resonance curves.

From the figure (6) we note that in superharmonic states, the resonance curve is linear and the amplitude increases as the external force amplitude E increases we note also, this amplitude deascreases as $a + 3b$ increases.

3.2.2 Subharmonic states

For the first subhamonic states $\Omega = 3 + \epsilon\sigma$, equating resonant terms at 0 from Eq.(31), we obtain:

$$2A' = A [1 - (a + 3b)|A|^2 - 2\Lambda^2(a + 3b\Omega^2)] + [a(2 - \Omega) + 3b\Omega] \bar{A}^2 \Lambda e^{j\epsilon\sigma T_0}. \quad (35)$$

Using (20) and after some algebraic manipulations, we rewrite (35) as follows

$$\begin{cases} p' = \frac{p}{2} \left[1 - \frac{p^2}{4}(a + 3b) - 2\Lambda^2(a + 3b\Omega^2) \right] + [a(2 - \Omega) + 3b\Omega] \frac{p^2\Omega}{4} \cos \varphi \\ \frac{\varphi' p}{3} - \frac{p\sigma}{3} = -[a(2 - \Omega) + 3b\Omega] \frac{p^2\Omega}{4} \sin \varphi, \text{ with } \varphi = \sigma T_1 - 3\theta. \end{cases} \quad (36)$$

The amplitude of oscillations of this subharmonic states ($p' = \varphi' = 0 \Leftrightarrow p = p_0, \varphi = \varphi_0$) is governed by the following nonlinear algebraic equation

$$\begin{cases} \frac{(a+3b)^2}{64} p_0^4 - \left(4\mu(a + 3b) + \Lambda^2 [a(2 - \Omega) + 3b\Omega]^2 \right) \frac{p_0^2}{16} + (\mu^2 + \frac{\sigma^2}{9}) = 0, \\ \text{with } \mu = \frac{1}{2} - \Lambda^2 (a + 3\Omega^2 b). \end{cases} \quad (37)$$

From the Fig. (7) we note a high sensibility of amplitude to the frequencie.

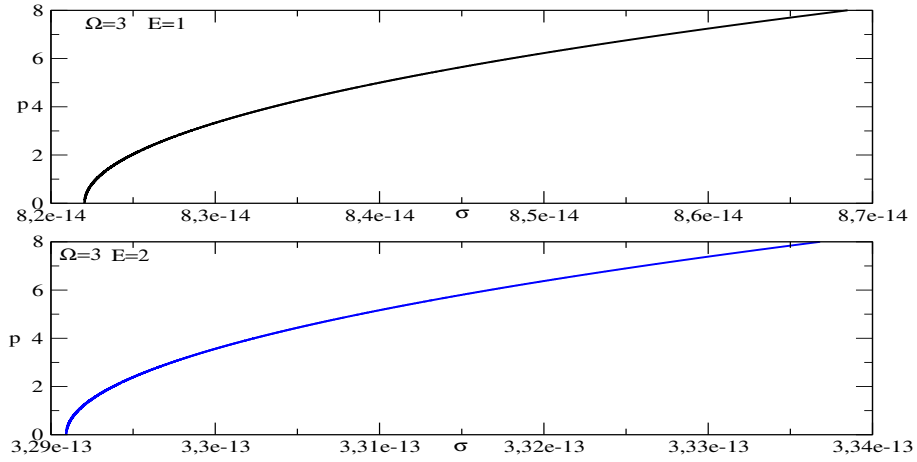


Figure 7: Effects of the parameters E on subharmonic resonance curves with $a = b = 1$.

4 Bifurcation and Chaotic behavior

The aim of this section is to find some bifurcation structures in the nonlinear dynamics of forced Van der Pol generalized oscillator described by equation (4) for resonant states since they are in interest for the system. For this purpose, we numerically solve this equation using the fourth-order Runge Kutta algorithm [17] and plot the resulting bifurcation diagrams and the variation of the corresponding largest Lyapunov exponent as the amplitude E , the parameters of nonlinearity a, b varied. The stroboscopic time period used to map various transitions which appear in the model is $T = \frac{2\pi}{\Omega}$.

The largest Lyapunov exponent which is used here as the instrument to measure the rate of chaos in the system is defined as

$$Lya = \lim_{t \rightarrow \infty} \frac{\ln \sqrt{dx^2 + d\dot{x}^2}}{t} \quad (38)$$

where dx and $d\dot{x}$ are respectively the variations of x and \dot{x} . Initial condition that we used in the simulations of this section is $(x_0, \dot{x}_0) = (1, 1)$. For the set of parameters $a = \{1, 6\}$, $b = \{1, 6\}$, $E = \{1, 6\}$, $\epsilon = \{0.01, 10\}$, $\Omega = \{1, \frac{1}{3}, 3\}$, the bifurcation and Lyapunov exponents diagrams for primary, superharmonic and subharmonic resonances are plotted respectively in Figs. (8), (9) and ((10), (11)). The bifurcation diagrams are in upper frame and its corresponding Lyapunov exponents are in lower frame. From the diagrams it is found that the model can switch from periodic to quasi-periodic, nonperiodic and chaotic oscillations. Since the model is highly sensitive to the initial conditions, it can leave a quasi-periodic state for a chaotic state without changing the physical parameters. Therefore, its basin of attraction has been plotted (see Figs.(16), (17)) in order to situate some regions of the initial conditions for which chaotic oscillations are observed. From these figures, we conclude that chaos is more abundant in the subharmonic resonant states than in the superharmonic and primary resonances. This confirms what has been obtained through their bifurcation diagrams and Lyapunov exponent.

We noticed that for the small value of ϵ the system is not chaotic.

In order to illustrate such situations, we have represented the various phase portraits using the parameters of the bifurcation diagram for which periodic, quasi-periodic and nonperiodic oscillations motions are observed in Figs. (12), (13), (14) and chaotic motions are observed in Fig.(15) for the two values of the parameters a, b, E above. From the phases diagram we observed appearance of the closed curve and the torus that confirm the two precedent types of motions predicted and the linear types of resonances seen in the third section.

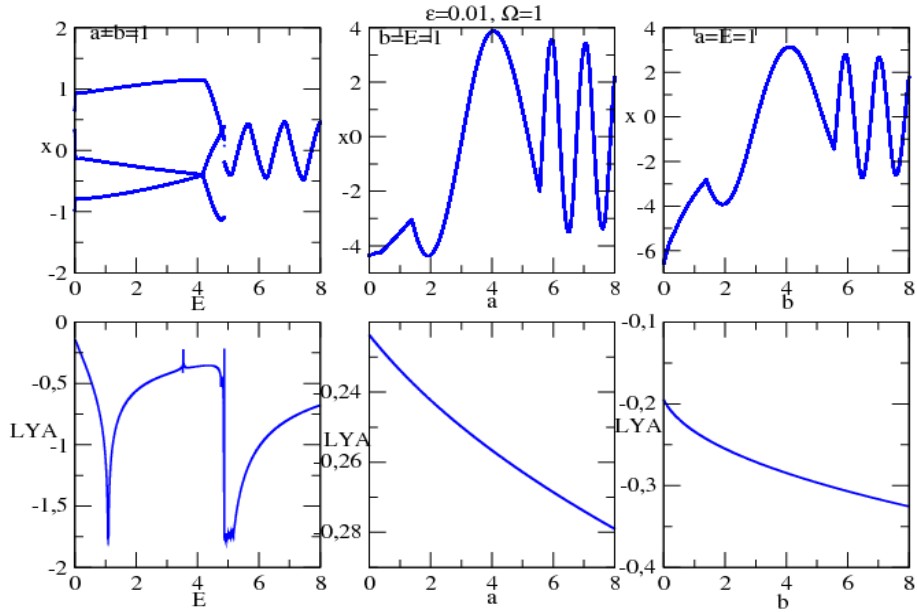


Figure 8: Bifurcation diagram (upper frame) and Lyapunov exponent (lower frame) for $\varepsilon = 0.01, \Omega = 1$ primary resonance case.

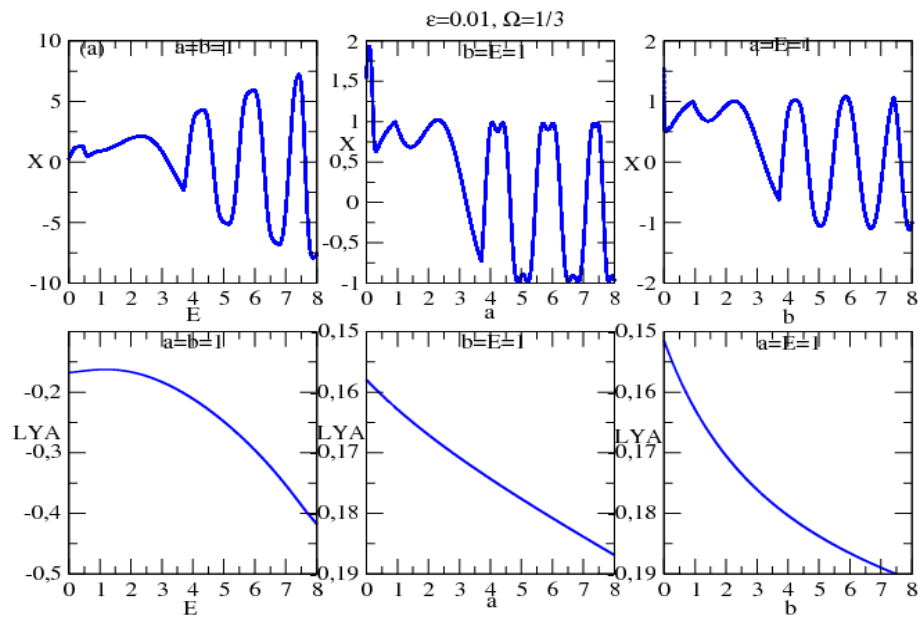


Figure 9: Bifurcation diagram (upper frame) and Lyapunov exponent (lower frame) for $\varepsilon = 0.01, \Omega = \frac{1}{3}$ supharmonic case.

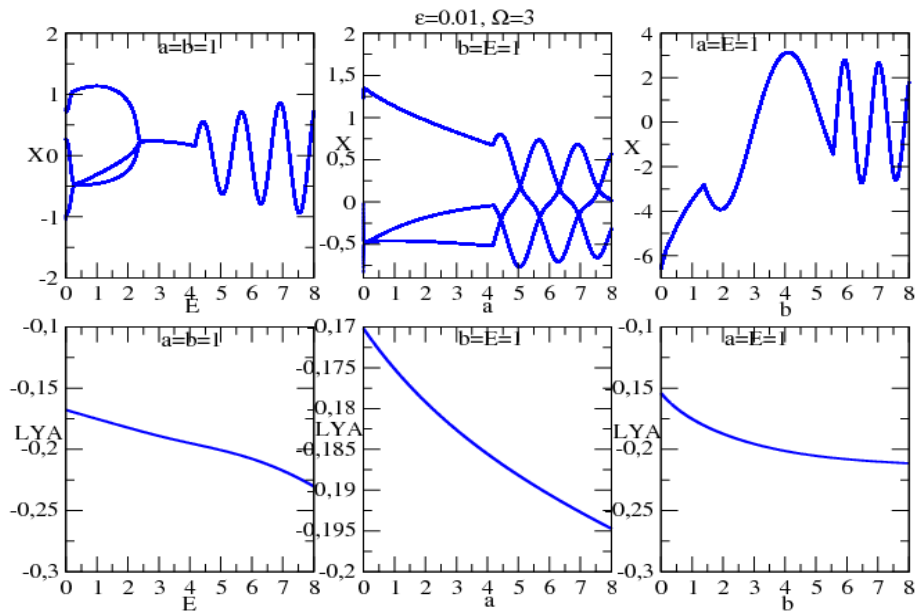


Figure 10: Bifurcation diagram (upper frame) and Lyapunov exponent (lower frame) for $\varepsilon = 0.01, \Omega = 3$ subharmonic case.

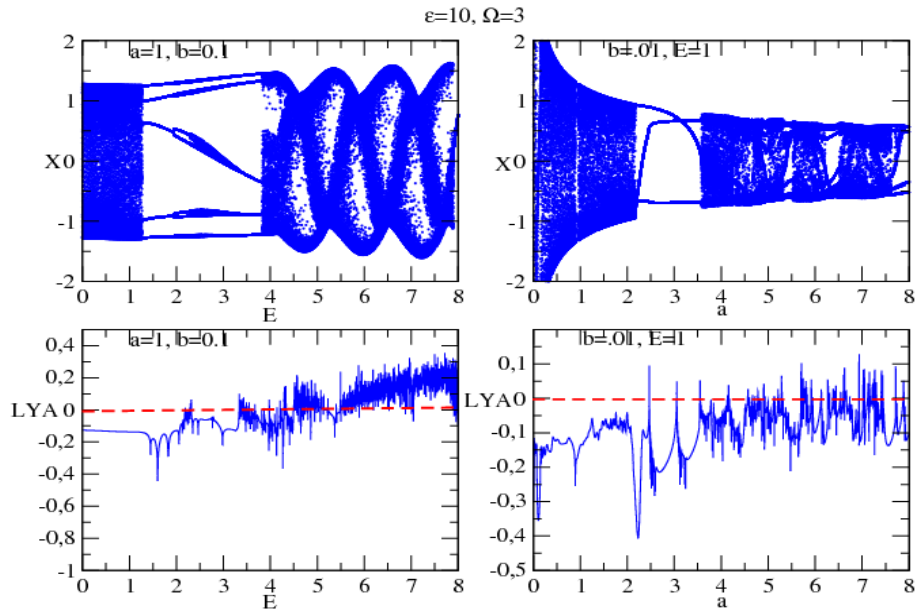


Figure 11: Bifurcation diagram (upper frame) and Lyapunov exponent (lower frame) for $\varepsilon = 10, \Omega = 3$ Subharmonic states case.

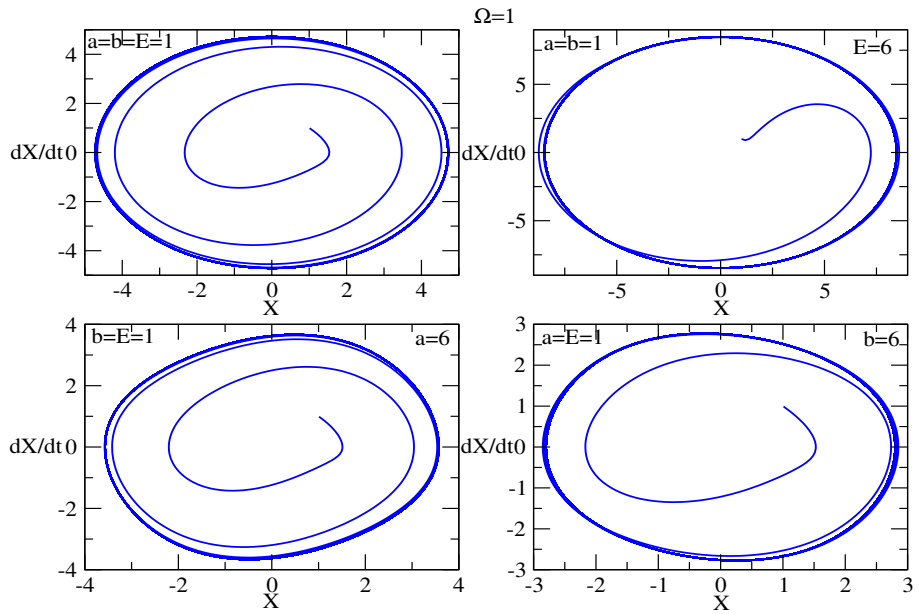


Figure 12: Phases diagram for parameters values in figure, $\varepsilon = 0.01$, primary resonance case.

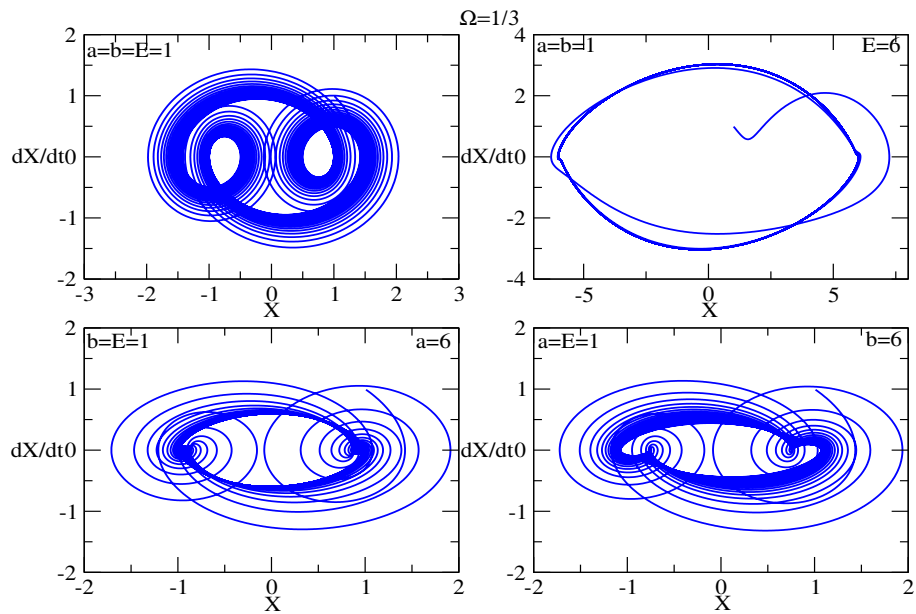


Figure 13: Phases diagram for parameters values in figure, $\varepsilon = 0.01$: Superharmonic states case.

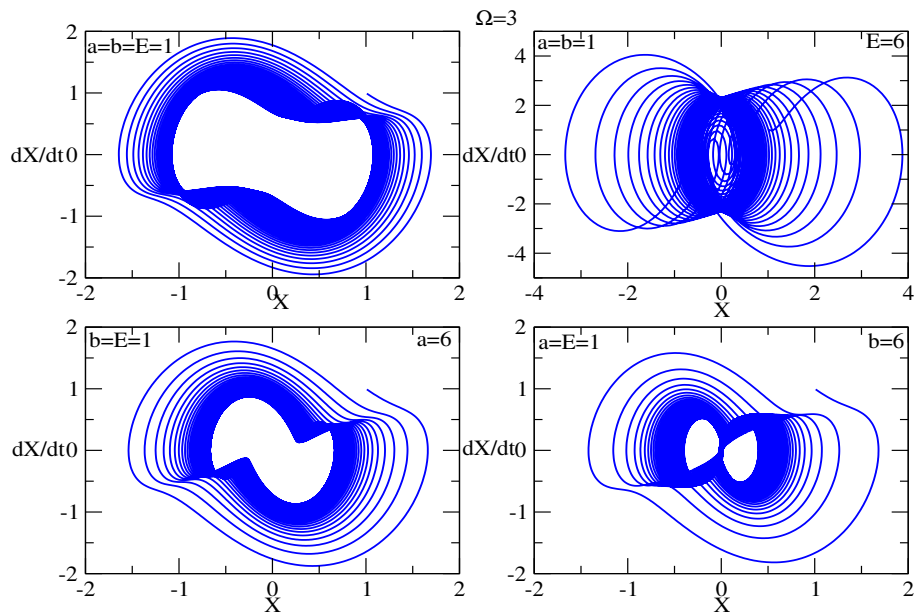


Figure 14: Phases diagram for parameters values in figure, $\varepsilon = 0.01$: Subharmonic states case.

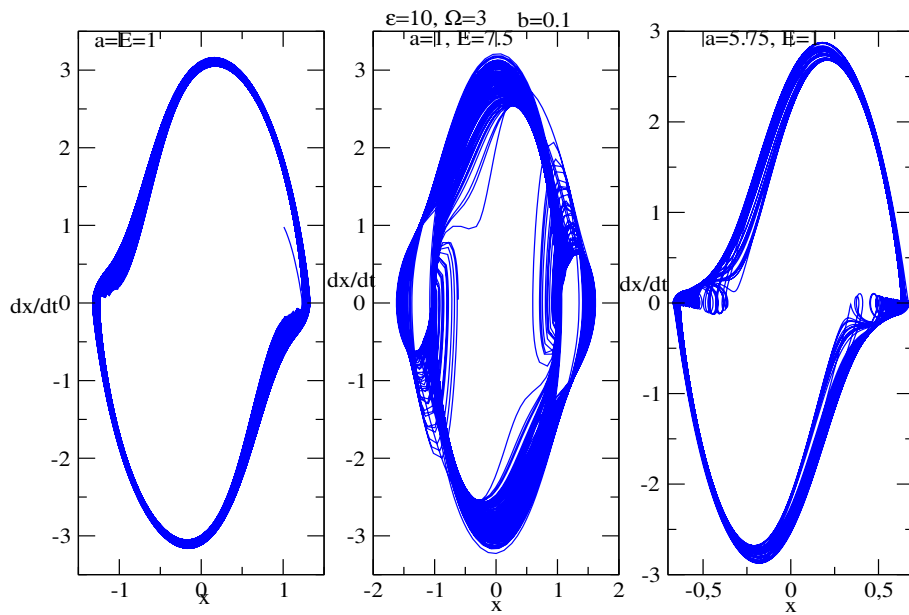


Figure 15: Phases diagram for parameters values in figure, $\varepsilon = 10, \Omega = 3$.

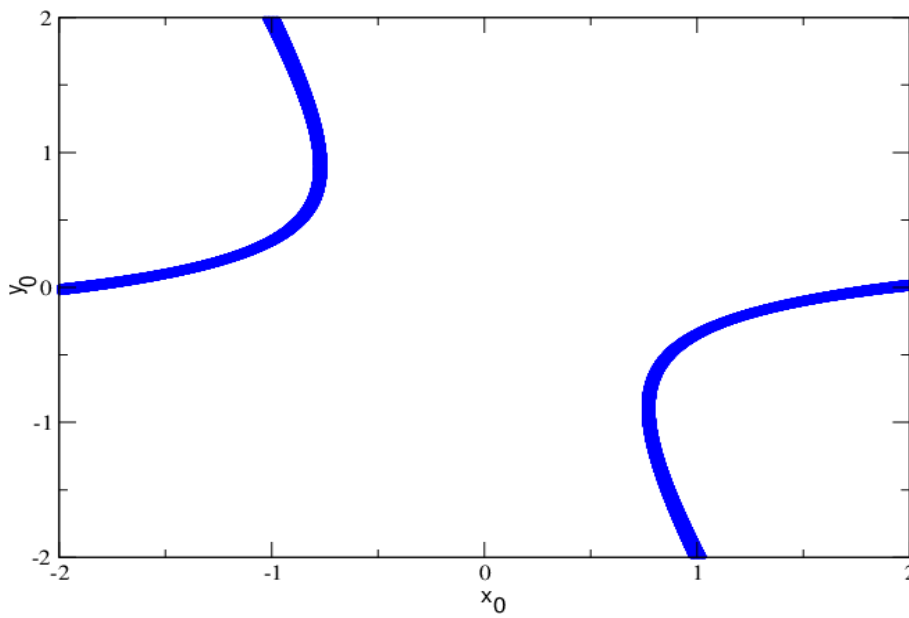


Figure 16: Chaoticity basin for parameters values in figure 9 with $E = 1$

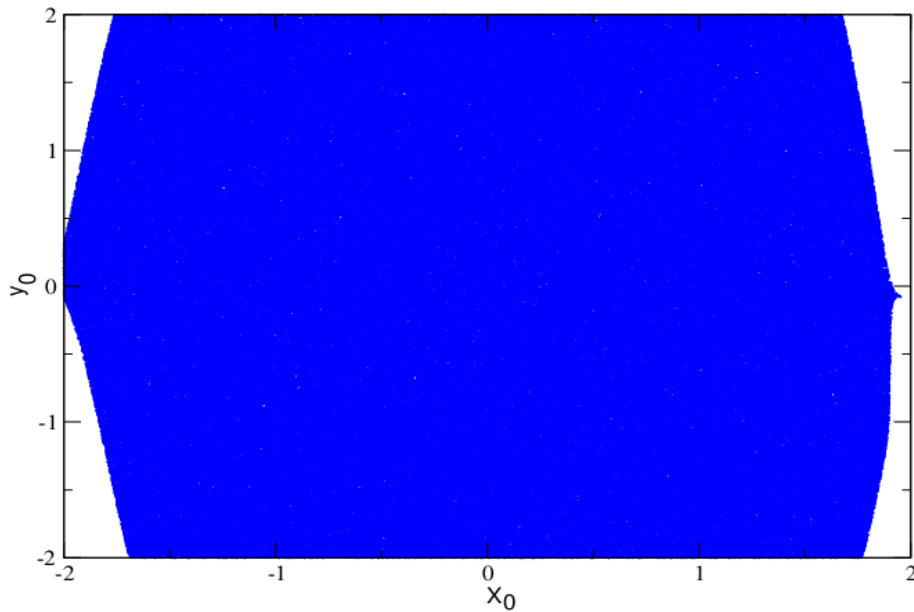


Figure 17: Chaoticity basin for parameters values in figure 11 with $E = 7.5$

5 Conclusion

In this work, we have studied the nonlinear dynamics for system oscillations modeled by forced Van der Pol generalized oscillator. In the harmonic case, the balance method has enabled us to derive the amplitude of harmonic oscillations, and the effects of the different parameters on the behaviors of model have been analyzed. For the resonant states case, the response amplitude, stability (for primary resonance case) have been derived by using multiple time-scales method and perturbation method. It appears the first-order superharmonic and subharmonic resonances. The effects of different parameters on these resonances are been found and we noticed that the Van der Pol, Rayleigh parameters and the external force amplitude have several action on the amplitude response and the resonances curves. The influences of these parameters on the resonant, hysteresis and jump phenomena have been highlighted. Our analytical results have been confirmed by numerical simulation. Various bifurcation structures showing different types of transitions from quasi-periodic motions to periodic and the beginning of chaotic motions have been drawn and the influences of different parameters on these motions have been study. It is noticed that behaviors of system have been controlled by the parameters a , b , E and but also the damping parameter ϵ . We conclude that chaos is more abundant in the subharmonic resonant states than in the superharmonic and primary resonances. This confirms what has been obtained through their bifurcation diagrams and Lyapunov exponent. The results show a way to predict admissible values of the signal amplitude for a corresponding set of parameters. This could be helpful for the experimentalists who are interested in trying to stabilize such a system with external forcing. For practical interests, it is useful to develop tools and to find ways to control or suppress such undesirable regions. This will be also useful to control high amplitude of oscillations obtained and which are generally source of instability in

physics system.

Acknowledgments

The authors thank IMSP-UAC and Benin government for financial support.

References

- [1] Gonze, D. and M. Kaufman. (2012) *Theory of non-linear dynamical systems*
- [2] Rajasekar, S., Parthasarathy, S., Lakshmanan M. (1992). *Prediction of horseshoe chaos in BVP and DVP oscillators*. Chaos, Solitons and Fractals 1992; 2 : 271.
- [3] Marios, Tsatsos. (2006). *Theoretical and Numerical Study of the Van der Pol equation* (Dissertation).
- [4] Van der Pol, B. (1920). *A theory of the amplitude of free and forced triode vibrations*. Radio Review, 1(1920), pp. 701 – 710, 754 – 762.
- [5] Van der Pol, B. (1926). *On relaxation-oscillations, The London, Edinburgh, and Dublin Philosophical Magazine and Journal of Science Ser.7, 2*, 978-992, 1926.
- [6] Appleton, E. V., and Van der Pol, B. (1921). *On the form of free triode vibrations, The London, Edinburgh, and Dublin Philosophical Magazine and Journal of Science Ser.6, 42*, 201-220, 1921.
- [7] Appleton E. V. and Van der Pol, B. (1922). *On a type of oscillation-hysteresis in a simple triode generator, The London, Edinburgh, and Dublin Philosophical Magazine and Journal of Science Ser.6, 43*, 177-193, 1922.
- [8] Van der Pol, B. (1922). *On oscillation hysteresis in a triode generator with two degrees of freedom, The London, Edinburgh, and Dublin Philosophical Magazine and Journal of Science Ser.6, 43*, 700 – 719, 1922.
- [9] Van der Pol, B. (1927). *Forced oscillations in a circuit with non-linear resistance (reception with reactive triode), The London, Edinburgh, and Dublin Philosophical Magazine and Journal of Science Ser.7, 3*, 65 – 80, 1927.
- [10] Van der Pol, B. and Van der Mark, J. (1927). *Frequency demultiplication, Nature*, 120, 363-364, 1927
- [11] Van der Pol, B. and Van der Mark, J. (1934). *The heartbeat considered as a relaxation oscillation, and an electrical model of the heart. The London, Edinburgh, and Dublin Philosophical Magazine and Journal of Science Ser.7, 6*, 763-775, (1928).
- [12] Van der Pol, B. (1934). *The nonlinear theory of electric oscillations, Proceedings of the Institute of Radio Engineers*, 22, 1051-1086, 1934.
- [13] Hinvi, A. L., Monwanou, A. V. and Chabi Orou, B. J. (2013). *A study of forced Van der Pol generalized oscillator with renormalization group method*.

- [14] de Pina Filho, A. C., and Dutra, M. S. (2009). *Application of hybrid Van der Pol-Rayleigh oscillators for modeling of a Bipedal robot.*
- [15] Hayashi, C. (1964). *Nonlinear Oscillations in Physical Systems*, (McGraw Hill, New York, 1964), Sec.1.5.
- [16] Nayfeh, A. H. (1981). *Introduction to perturbation techniques*, (John Wiley and Sons, New York, 1981), Sec.4.5.
- [17] Piskunov, N. (1980). *Calcul Différentiel et intégral*, Tome II, 9^e edition, MIR, Moscou (1980).